

EPR study of the Jahn-Teller effect of Cu^{2+} in $\text{ZnTiF}_6 \cdot 6\text{H}_2\text{O}$

D. K. De, R. S. Rubins, and T. D. Black

Department of Physics, Box 19059, The University of Texas at Arlington, Arlington, Texas 76019

(Received 16 August 1982)

The 34-GHz EPR spectrum of Cu^{2+} in $\text{ZnTiF}_6 \cdot 6\text{H}_2\text{O}$ shows a Jahn-Teller effect with a transition from a single-line spectrum at high temperatures to a multiline anisotropic spectrum. The transition temperature on cooling varied with Cu concentration from 172 K for a sample containing 0.2 at. % Cu to roughly 90 K for a 46-at. % Cu sample. For dilute samples, the single-line spectrum was isotropic at 300 K with $g = 2.223 \pm 0.005$, but showed axial symmetry about the trigonal axis at 180 K with $g_{\parallel} = 2.226 \pm 0.005$ and $g_{\perp} = 2.223 \pm 0.005$. At 4.2 K, a "static" Jahn-Teller effect was observed with six axially symmetric Cu^{2+} spectra, each with $g_{\parallel} = 2.470 \pm 0.005$, $g_{\perp} = 2.100 \pm 0.005$, $|A_{\parallel}| \approx 106 \times 10^{-4} \text{ cm}^{-1}$, and $|A_{\perp}| \approx 30 \times 10^{-4} \text{ cm}^{-1}$. The z axis of these spectra was found to lie along the fourfold axes of two cubes with a common [111] axis, rotated by $40^\circ \pm 2^\circ$ with respect to each other about this axis. Analysis of the 4.2-K data leads to the values $q \approx 0.50$ for the Ham reduction factor and $\kappa \approx 0.26$ for the Fermi contact parameter, with $A_{\parallel}A_{\perp} < 0$. An activation energy of about 100 cm^{-1} was deduced from the gradual increase of the anisotropy of the spectrum on cooling in the low-temperature region.

I. INTRODUCTION

The Jahn-Teller effect is associated with ions in symmetrical or nearly symmetrical configurations having orbitally degenerate ground states.¹ The coupling of the degenerate states of the ion with the appropriate lattice modes results in asymmetric displacements of the nuclei which lift the orbital degeneracies. Electron paramagnetic resonance (EPR) has been an effective tool for studying the Jahn-Teller effect and, in the work of Bleaney *et al.*²⁻⁴ on Cu^{2+} in $\text{ZnSiF}_6 \cdot 6\text{H}_2\text{O}$, provided its first unambiguous experimental verification. In $\text{ZnSiF}_6 \cdot 6\text{H}_2\text{O}$, the Zn^{2+} ion is surrounded by a regular octahedron of water molecules,⁵ although the crystal as a whole has trigonal symmetry.⁶ The twofold orbital degeneracy of the 2E ground state of a substitutional Cu^{2+} ion is not removed by the trigonal component of the crystal field, so that a Jahn-Teller effect occurs. At low temperatures, three axially symmetric Cu^{2+} spectra, corresponding to distortions of the water octahedra along the three fourfold axes of the cube, are observed. This situation is referred to as a "static" Jahn-Teller effect. The nearly isotropic spectrum observed at higher temperatures was explained by Abragam and Pryce⁷ as a dynamical averaging of the individual lines of the static effect. Following two decades of theoretical development, Dang, Buisson, and Williams⁸ made a detailed experimental and theoretical study of $\text{ZnSiF}_6 \cdot 6\text{H}_2\text{O}:\text{Cu}^{2+}$ between 1.2 and 80 K, emphasizing line shapes, relaxation rates, and the evolution of the EPR spectrum with temperature. The effect of the small trigonal component of the crystal field on the EPR spectrum was also considered.

In this paper we present an EPR study at 35 GHz of Cu^{2+} in single crystals of $\text{ZnTiF}_6 \cdot 6\text{H}_2\text{O}$ in the temperature range 300–2 K with particular emphasis on the analysis of the 4.2-K spectrum. Single crystals of $(\text{Zn,Cu})\text{TiF}_6 \cdot 6\text{H}_2\text{O}$ of various Cu concentrations were

grown from aqueous solution at room temperature. The EPR measurements were made on a $K\alpha$ band spectrometer of conventional design.

Although the room-temperature structures of $\text{ZnSiF}_6 \cdot 6\text{H}_2\text{O}$ and $\text{ZnTiF}_6 \cdot 6\text{H}_2\text{O}$ are related,⁶ the latter appears to be isomorphous with $\text{MgSiF}_6 \cdot 6\text{H}_2\text{O}$ (Ref. 9) and $\text{FeSiF}_6 \cdot 6\text{H}_2\text{O}$,¹⁰ which have two inequivalent metal-ion sites related by a mirror plane containing the symmetry axis. On cooling, there is a phase transition from the trigonal space group D_{3d}^5 ($R\bar{3}m$) to the monoclinic group C_{2h}^5 ($P2_1/c$).⁹ Nuclear magnetic resonance (NMR) studies of the ${}^{19}\text{F}$ nuclei in pure $\text{ZnTiF}_6 \cdot 6\text{H}_2\text{O}$ have established the transition temperature to be $182 \pm 1 \text{ K}$.¹¹ In the low-temperature (monoclinic) phase, EPR measurements on Ni^{2+} in $\text{ZnTiF}_6 \cdot 6\text{H}_2\text{O}$ have indicated the presence of six inequivalent magnetic sites, with spectra that coincide along the c (pseudotrigonal) axis.¹² In the plane perpendicular to the c axis, the spectra reduce to two sets of three lines, each set showing a 60° rotational symmetry. The monoclinic distortions are small in these crystals. As a result, the z axis of the six inequivalent spectra for "non-Jahn-Teller" ions such as Ni^{2+} and Fe^{2+} lie within a few degrees of the crystal c axis.¹²⁻¹⁵ The magnitude of the monoclinic distortion, as given by the orthorhombic component of the spin Hamiltonian, increases with temperature until the phase transition is reached.

In contrast to the above, the z axes of the six inequivalent spectra observed for Cu^{2+} in $\text{ZnTiF}_6 \cdot 6\text{H}_2\text{O}$ at 4.2 K lie along the three fourfold axes of two cubes sharing a common [111] axis, as will be discussed in Sec. II C. Apart from the existence of two Cu^{2+} ions per unit cell, the EPR spectrum in $\text{ZnTiF}_6 \cdot 6\text{H}_2\text{O}$ at 4.2 K is essentially similar to that observed in $\text{ZnSiF}_6 \cdot 6\text{H}_2\text{O}$, both with respect to the orientations of the z axes and the principal values of the g tensor (see Sec. III). A comparable six-ion spectrum in cupric insulin crystals was likewise attributed to a Jahn-Teller effect.¹⁶ However, the most direct evi-

dence for the existence of a Jahn-Teller effect in $\text{ZnTiF}_6 \cdot 6\text{H}_2\text{O}$ in the monoclinic phase is provided by the temperature evolution of the low-temperature EPR spectrum. The gradual reduction of anisotropy observed with increasing temperature, which is illustrated in Fig. 1, cannot be explained by a weak orthorhombic crystal-field term, which would have only a marginal effect on the principal g values of Cu^{2+} ions in predominantly cubic octahedral surroundings.¹⁷ On the other hand, the temperature evolution of the EPR spectrum follows naturally from the temperature dependence of the reorientation rate, as discussed qualitatively in Sec. III.

While detailed analysis of the 4.2-K spectrum in terms of the Jahn-Teller effect forms the central part of this study, there are other aspects which pose problems of theoretical interest. One such problem is the modification of the Jahn-Teller effect by the structural phase transition. Our data show that the transition on cooling from a single-line to a multiline spectrum occurs at a temperature which is strongly concentration dependent and appreciably below that of the phase transition in the pure material. A second problem is that of the temperature evolution of the Jahn-Teller spectrum above 4.2 K, where the gradual decrease in anisotropy contrasts sharply with the more complicated effects observed in $\text{ZnSiF}_6 \cdot 6\text{H}_2\text{O}$.⁸

In the following section, brief descriptions of the transition and high-temperature region precede a more detailed analysis of the 4.2-K spectrum. The discussion (Sec. III) deals with the evaluation of Jahn-Teller and hyperfine structure parameters from the 4.2-K data, followed by a simple interpretation of the gradual decrease of anisotropy with increase of temperature in terms of a single anisotropy parameter $u(T)$.

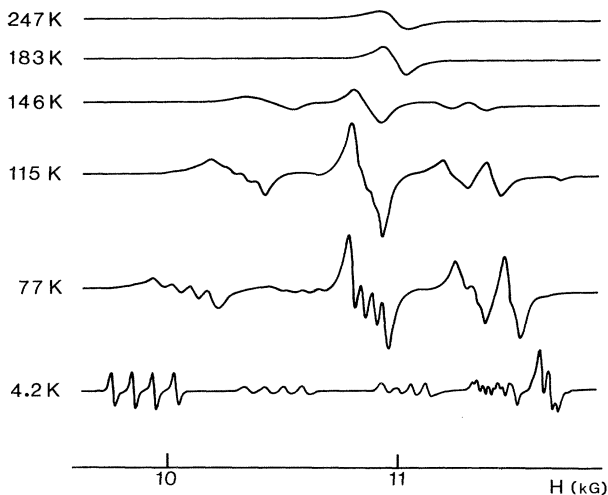


FIG. 1. Evaluation of the EPR spectrum at 34 GHz between room temperature and 4.2 K for an orientation in plane 2 giving the maximum line separations.

II. EXPERIMENTAL RESULTS

A. Transition

At high temperatures, a single-line EPR spectrum without structure was observed at all orientations. As the crystal was cooled slowly, a transition occurred in which the high-temperature spectrum was replaced by an anisotropic spectrum composed of several lines. The temperature of this transition was below that of the phase transition of 182 K measured in pure $\text{ZnTiF}_6 \cdot 6\text{H}_2\text{O}$,¹¹ and showed a marked dependence on Cu concentration, varying from 172 K for a 0.2-at. % sample to approximately 92 K for a 46-at. % sample.¹⁸ For samples of low Cu concentration, the transition was relatively sharp. For example, in an experiment in which the cooling rate was 3°C/h, the high- and low-temperature spectra coexisted for about 10 min. On the other hand, in the very concentrated samples, the transition extended over a range of about 10°C. The concentration dependence of the transition is the subject of a separate study by these authors, and will not be considered further in this paper. The measurements discussed in the remainder of this paper refer to the most dilute samples of approximately 0.2-at. % Cu concentration.

B. High-temperature spectrum

At room temperature, the single-line spectrum was isotropic with a g value and a peak-to-peak linewidth ΔH (in G) given by

$$g = 2.22 \pm 0.01, \quad \Delta H \simeq 170.$$

In the region just above the transition, both the g value and linewidth showed an anisotropy about the c axis of crystal. At 180 K, the following values were obtained:

$$g_{\parallel} = 2.226 \pm 0.005, \quad \Delta H \simeq 85,$$

$$g'_{\perp} = 2.223 \pm 0.005, \quad \Delta H \simeq 110,$$

with ΔH in G, and

$$g_{\parallel} - g'_{\perp} = 0.003 \pm 0.001.$$

This anisotropy is both smaller and of the opposite sign to that observed in $\text{ZnSiF}_6 \cdot 6\text{H}_2\text{O}$ at 77 K.⁶

The spin-lattice relaxation time T_1 , was calculated from the increase of the linewidth with temperature and fitted to an Orbach relaxation process via an excited state roughly 1400 cm^{-1} above the ground. This value is of the same order as those observed by Müller *et al.*¹⁹ for a number of Jahn-Teller systems, and interpreted in terms of relaxation via a centrifugally stabilized state on the upper potential branch.²⁰

C. Low-temperature spectra

The EPR spectra below the transition temperature became increasingly anisotropic as the temperature was lowered. A nearly resolved Cu^{2+} hyperfine structure ($I = \frac{3}{2}$) was observed in the low-field EPR lines below 120 K, although the abundant isotopes Cu^{63} and Cu^{65} could

TABLE I. Spin-Hamiltonian parameters for Cu^{2+} in $\text{ZnTiF}_6 \cdot 6\text{H}_2\text{O}$ in plane 1 below the transition. (Plane 1 is a natural hexagonal face of the crystal containing the c axis.)

Orientation	Temperature (K)	g	A (G)
c axis	77	2.230 ± 0.005	52 ± 2
	4.2	2.230 ± 0.005	64 ± 2
Maximum g	125	2.36 ± 0.01	57 ± 3
	96	2.39 ± 0.01	70 ± 3
	77	2.411 ± 0.005	77 ± 2
Minimum g	4.2	2.443 ± 0.005	90 ± 2
	166	2.16 ± 0.01	
	142	2.15 ± 0.01	
	125	2.14 ± 0.01	
	96	2.13 ± 0.01	
	77	2.13 ± 0.01	
	4.2	2.10 ± 0.01	$\approx 30^a$

^aHyperfine structure was unevenly spaced and the line shapes were asymmetrical.

not be distinguished because of the linewidths. At 77 K, the spectrum consisted of at least four inequivalent Cu^{2+} lines. At 4.2 K, six inequivalent Cu^{2+} lines (each with hyperfine structure) were clearly observed in suitable orientations of the crystal. No further lineshifts were observed below 4.2 K.

The EPR measurements were made in three mutually perpendicular crystal planes, designated as follows.

(i) Plane 1, in which a natural hexagonal face of the crystal, containing the c axis, was horizontal (i.e., in the plane of rotation of the external magnetic field).

(ii) Plane 2, which was obtained from plane 1 by a rotation of 90° about the c axis.

(iii) Plane 3, in which the c axis was vertical.

The highest and lowest values of the g and A tensors for the three planes and their values parallel to the c axis (for planes 1 and 2) are given as functions of temperature in Tables I–III. The development of the EPR spectrum on cooling is shown in Fig. 1 for a particular orientation in plane 2 in which the anisotropic spectrum has its max-

imum spread. The six inequivalent Cu^{2+} spectra may be seen at 4.2 K.

The spectra at 4.2 K were studied in some detail. The centers of each group of hyperfine lines were measured at 5° intervals in each of the three planes and compared with a simple theory based on the estimates of the extreme g values for each site and the spatial orientations of the z axes as outlined below. The results are shown in Figs. 2–4. In plane 1, the six Cu^{2+} spectra were equivalent in pairs. Experimentally, the coincidence was not quite exact, but this was attributed to a slight misorientation of the crystal. In planes 2 and 3, six distinct Cu^{2+} spectra could be observed. In plane 3, these could be divided into two groups of three spectra each with minima (in field) 60° apart. The angular separation of the two groups was either $20^\circ \pm 2^\circ$ or $40^\circ \pm 2^\circ$. If the orientation $\phi = 0^\circ$ was assumed to correspond to a direction parallel to a hexagonal crystal face, then the minima occurred near the angles 10° , 50° , 70° , 110° , 130° , and 170° . The maximum g values in plane 3 varied between 2.353 ± 0.005 and 2.364 ± 0.005 .

TABLE II. Spin-Hamiltonian parameter for Cu^{2+} in $\text{ZnTiF}_6 \cdot 6\text{H}_2\text{O}$ in plane 2 below the transition. (Plane 2 is a plane containing the c axis which is perpendicular to a natural hexagonal face of the crystal.)

Orientation	Temperature (K)	g	A (G)
c axis	150	2.228 ± 0.005	
	77	2.228 ± 0.005	50 ± 2
	4.2	2.228 ± 0.005	63 ± 2
Maximum g	146	2.33 ± 0.01	49 ± 3
	115	2.36 ± 0.01	63 ± 3
	77	2.41 ± 0.01	78 ± 2
	4.2	2.457 ± 0.005	92 ± 2
Minimum g	146	2.15 ± 0.01	
	115	2.14 ± 0.01	
	77	2.12 ± 0.01	
	4.2	2.10 ± 0.01	$\approx 32^a$

^aHyperfine structure was unevenly spaced and the line shapes were asymmetrical.

TABLE III. Spin-Hamiltonian parameters for Cu^{2+} in $\text{ZnTiF}_6 \cdot 6\text{H}_2\text{O}$ in plane 3 below the transition. (Plane 3 is the plane perpendicular to the c axis.)

Orientation	Temperature (K)	g^a	A (G)
Maximum g	77	2.32 ± 0.01	67 ± 2
	4.2	2.36 ± 0.01	87 ± 2
Minimum g	77	2.13 ± 0.01	
	4.2	2.10 ± 0.01	$\approx 26^b$

^aMean values for the six inequivalent Cu^{2+} spectra are given (see text).

^bHyperfine structure was unevenly spaced and the line shapes were asymmetrical.

The difference was probably due to a crystal misalignment, and an average value is quoted in Table III. In each plane, the hyperfine structure was approximately symmetrical at each low-field extremum, with uniform spacings of about 90 G and linewidths in the range 30–40 G. On the other hand, the line shapes were asymmetrical and the spacings were uneven at each high-field extremum. The linewidths at the high-field extrema were roughly half those at low fields.

The theoretical model used to fit the 4.2-K data is related to that used by Bleaney *et al.*,^{2,4} to fit the low-temperature data in $\text{ZnSiF}_6 \cdot 6\text{H}_2\text{O}$, where three spectra of axial symmetry were attributed to static Jahn-Teller distortions along each of the three fourfold axes of a cube. In the case of $\text{ZnTiF}_6 \cdot 6\text{H}_2\text{O}$, the two sets of three Cu^{2+} spectra observed in plane 3 correspond to two cubes rotated with respect to each other by an angle of approximately 20° or 40° . A qualitative fit of the data in planes 1 and 2 can be made only for the rotation angle of 40° . A schematic diagram of the model is shown in Fig. 5, which represents the projections of the z axes of the six Cu^{2+} spectra onto plane 3. The intersections of this plane with

planes 1 and 2 are noted. Assuming that the distortions from cubic symmetry were small, so that the angle between the z axis of each spectrum and the c axis of the crystal was approximately 55° , a reasonable fit of the 4.2-K data was obtained for the values

$$g_{\parallel} = 2.470 \pm 0.005, \quad |A_{\parallel}| = (106 \pm 2) \times 10^{-4},$$

$$g_{\perp} = 2.100 \pm 0.005, \quad |A_{\perp}| = (30 \pm 2) \times 10^{-4},$$

with A_{\parallel} and A_{\perp} in cm^{-1} . While the signs of A_{\parallel} and A_{\perp} could not be determined directly from these measurements, only the assumption of opposite signs for A_{\parallel} and A_{\perp} lead to a reasonable value for the Fermi-contact term in the hyperfine splitting, and to agreement with the temperature dependencies of A_{\parallel} and A_{\perp} , as discussed in Sec. III of this paper.

The theoretical fit of the data, as shown by the solid curves in Figs. 2–4, is good enough to indicate the basic correctness of the model. The discrepancies observed in some of the curves in planes 1 and 2 may be due in part to slight experimental misalignments of the crystal and to nonaxial g tensors arising from the trigonal and monoclin-

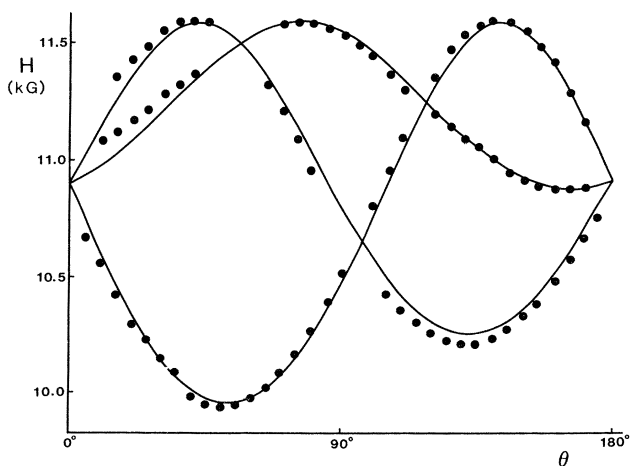


FIG. 2. Observed and calculated angular variations of the mean resonance fields of each set of Cu^{2+} hyperfine lines at 34 GHz in plane 1 at 4.2 K. Points represent the experimental data and solid curves the calculated values. Angles $\theta = 0^\circ$ or 180° correspond to the c axis.

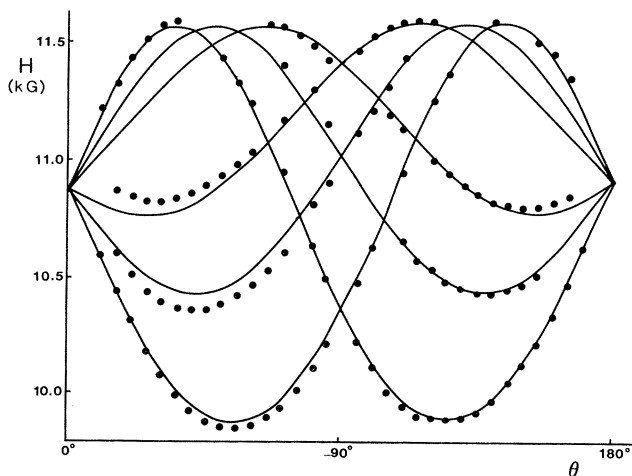


FIG. 3. Observed and calculated angular variations of the mean resonance fields of each set of Cu^{2+} hyperfine lines at 34 GHz in plane 2 at 4.2 K. Points represent the experimental data and solid curves the calculated values. Angles $\theta = 0^\circ$ or 180° correspond to the c axis.

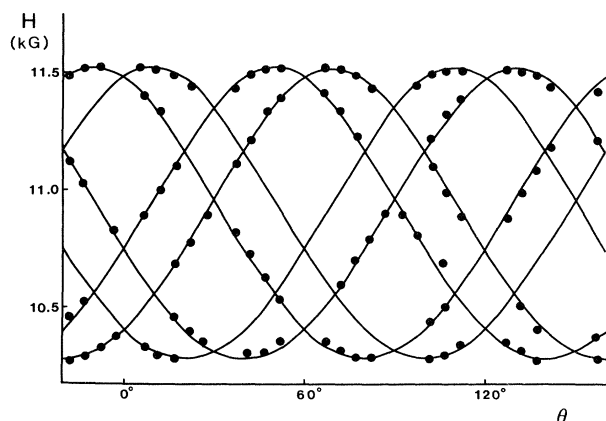


FIG. 4. Observed and calculated angular variations of the mean resonance fields of each set of Cu^{2+} hyperfine lines at 34 GHz in plane 3 at 4.2 K. Points represent the experimental data and solid curves the calculated values. Angles $\theta=0^\circ$, 60° , and 120° correspond to directions perpendicular to hexagonal crystal faces.

ic components of the crystal field, which were ignored in the simple model used.

III. DISCUSSION

The $\text{Cu}^{2+}(\text{H}_2\text{O})_6$ complex in $\text{ZnTiF}_6 \cdot 6\text{H}_2\text{O}$, like that in $\text{ZnSiF}_6 \cdot 6\text{H}_2\text{O}$, is subject to a static Jahn-Teller effect at low temperatures. It may be seen from Table IV that the principal g values are similar for the two materials, both in the low- and high-temperature regimes (apart from opposing signs for $g'_{||} - g'_\perp$). However, significant differences exist. In $\text{ZnTiF}_6 \cdot 6\text{H}_2\text{O}$, the 4.2-K EPR spectra correspond to two Jahn-Teller ions per unit cell, giving six inequivalent Cu^{2+} spectra, as opposed to just three in $\text{ZnSiF}_6 \cdot 6\text{H}_2\text{O}$. Also, the anisotropic spectra are observed to much higher temperatures in $\text{ZnTiF}_6 \cdot 6\text{H}_2\text{O}$, almost to the structural transition temperature of 182 K in the most dilute samples. Notably absent were features of the $\text{ZnSiF}_6 \cdot 6\text{H}_2\text{O}$ spectra described by Dang *et al.*,⁸ such as the coexistence of two spectra in the [111] direction between 8 and 27 K and the visibility of the “perpendicular”

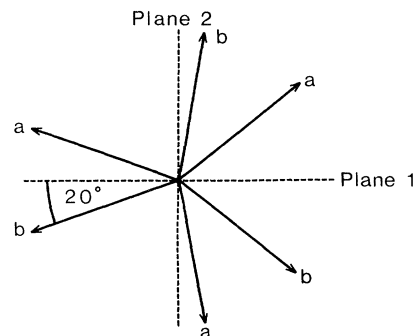


FIG. 5. Projections of the fourfold axes of the “static” Jahn-Teller distortion onto plane 3. The two cubes, which are labeled a and b , are rotated about a common [111] axis by approximately 40° . Intersections of plane 3 with planes 1 and 2 are shown.

group of lines to higher temperatures than the “parallel” group in the [100] direction.

The key feature of the Cu^{2+} spectrum in $\text{ZnTiF}_6 \cdot 6\text{H}_2\text{O}$ on cooling from room temperature was the replacement of the single nearly isotropic line by an anisotropic spectrum which showed a gradual increase of anisotropy down to 4.2 K.

The experimentally determined values of $g_{||}$, g_\perp , $A_{||}$, and A_\perp at 4.2 K were used to derive other parameters of the system. Following Ham¹ and Boatner *et al.*,²¹ the parameters g_1 , qg_2 , A_1 , and qA_2 may be determined from the equations

$$g_{||} = g_1 + 2qg_2, \quad g_\perp = g_1 - qg_2, \quad (1)$$

$$A_{||} = A_1 + 2qA_2, \quad A_\perp = A_1 - qA_2, \quad (2)$$

provided that the relative signs of A_1 and A_2 are known. The parameter g_2 and the orbital reduction factor α^2 may be estimated from the following equations given by Boatner *et al.*:²¹

$$g_1 = g_e - 4\alpha^2\lambda/\Delta - (4 + \alpha^2)\lambda^2/\Delta^2, \quad (3)$$

$$g_2 = -4\alpha^2\lambda/\Delta + (2 - 4\alpha^2)\lambda^2/\Delta^2, \quad (4)$$

where g_e is the free-electron g value, $\lambda \simeq -830 \text{ cm}^{-1}$ is the spin-orbit coupling constant of the free ion, Δ is the cubic

TABLE IV. Comparison of EPR data for Cu^{2+} in $\text{ZnTiF}_6 \cdot 6\text{H}_2\text{O}$ and $\text{ZnSiF}_6 \cdot 6\text{H}_2\text{O}$.

Crystal	Temperature	(a) High-temperature spectra ^a				Reference
		$g'_{ }$	g'_\perp	$ A'_{ } $ (10^{-4} cm^{-1})	$ A'_\perp $ (10^{-4} cm^{-1})	
$\text{ZnTiF}_6 \cdot 6\text{H}_2\text{O}$	300	2.223	2.223			This work
	180	2.226	2.223			This work
$\text{ZnSiF}_6 \cdot 6\text{H}_2\text{O}$	90	2.221	2.230	21	28	Ref. 4
(b) Low-temperature spectra						
$\text{ZnTiF}_6 \cdot 6\text{H}_2\text{O}$	4.2	2.470	2.100	106 ^b	30	This work
$\text{ZnSiF}_6 \cdot 6\text{H}_2\text{O}$	4.2	2.460	2.100	107 ^b	14	Ref. 8

^a $g'_{||}$, g'_\perp , $A'_{||}$, and A'_\perp refer to spectra with axial symmetry about the trigonal axis.

^b $A_{||}A_\perp < 0$.

field splitting of the 2D ground state of the free Cu^{2+} ion, and α is the metal d -orbit coefficient in the normalized ground state,²² which may be written

$$\psi_g = \alpha d_{x^2-y^2} - (\alpha'/2)(-\sigma_x^{(1)} + \sigma_y^{(2)} + \sigma_x^{(3)} - \sigma_y^{(4)}), \quad (5)$$

where $d_{x^2-y^2}$ refers to a Cu^{2+} d orbital and σ_x and σ_y refer to hybridized ligand orbitals. In the approach adopted here, α^2 and g_2 were calculated from Eqs. (3) and (4) by assuming a value for the factor λ/Δ . Taking a value for Δ of 12000 cm^{-1} , which lies between the value measured optically for Cu^{2+} in $\text{ZnSiF}_6 \cdot 6\text{H}_2\text{O}$ (Ref. 23) and that for the $[\text{Cu} \cdot 6\text{H}_2\text{O}]^{2+}$ complex in solution,²⁴ the factor λ/Δ is approximately -0.069 . From Eqs. (3) and (4), it may be seen that the difference $g_1 - g_2$ does not contain this factor in the first order, so that only the parameter α^2 is sensitive to the value assumed for Δ .

The Ham reduction factor q may be obtained from the knowledge of both qg_2 and g_2 . A list of the parameters determined so far is given in part (b) of Table V. The value found for q of 0.50 corresponds to the strong Jahn-Teller limit $E_{JT} \gg \hbar\omega$.¹

In dealing with the hyperfine structure, we have assumed q to be exactly 0.5, so that the expressions for $A_{||}$ and A_{\perp} revert to those for an octahedral field with a tetragonal distortion; i.e.,^{22,25,26}

$$A_{||} \simeq P[-(4\alpha^2/7) - \kappa + (g_{||} - g_e) + (\frac{3}{7})(g_{\perp} - g_e)], \quad (6)$$

$$A_{\perp} \simeq P[(2\alpha^2/7) - \kappa + (\frac{11}{14})(g_{\perp} - g_e)], \quad (7)$$

where $P = g_e g_n \beta \beta_n \langle r^{-3} \rangle$, g_n is the nuclear g factor, β and β_n are the Bohr and nuclear magnetons, respectively, κ is the Fermi-contact parameter, $\langle r^{-3} \rangle$ is the expectation value of r^{-3} for free-ion d electrons, and covalency parameters other than α^2 have been omitted. According to Kivelson and Neiman,²⁵ $\kappa = \alpha^2 \kappa_0$, where κ_0 is the free-ion parameter which was estimated by Abragam and Pryce⁷ to be 0.36.

The values deduced for A_1 , A_2 , P , and κ are given in part (b) of Table V for both relative signs of $A_{||}$ and A_{\perp} . For simplicity in presenting the data, $A_{||}$ has been assumed to be negative, consistent with the sign determinations of Bleaney *et al.*^{4,27} for other hydrated salts. Only when $A_{||}A_{\perp} < 0$ is the value obtained for κ reasonable; i.e.,

$\kappa < \kappa_0 (=0.36)$. The value of $420 \times 10^{-4} \text{ cm}^{-1}$ obtained for P in this case is somewhat larger than that of $360 \times 10^{-4} \text{ cm}^{-1}$ deduced by Abragam and Pryce⁷ for the free ion. However, it should be noted that the value obtained for P , but not that for κ , is very sensitive to the value used for Δ . For example, increasing Δ from 12000 to 12300 cm^{-1} would decrease P from 420×10^{-4} to $390 \times 10^{-4} \text{ cm}^{-1}$ (and increase α^2 from 0.88 to 0.91) without changing κ . The conclusion $A_{||}A_{\perp} < 0$ agrees with that deduced by Dang *et al.*⁸ by a different method for $\text{ZnSiF}_6 \cdot 6\text{H}_2\text{O}$.

The gradual increase of the anisotropy and hyperfine splitting of the spectrum on cooling the crystal in the low-temperature phase, which is illustrated in Fig. 1 (see also Tables I and II), may be interpreted in a simple manner by means of an anisotropy parameter $u(T)$, the difference of which from unity represents the delocalization of the Cu^{2+} ions. In the case of strong Jahn-Teller coupling ($q = \frac{1}{2}$), this parameter plays essentially the same role as the zero-point vibrational parameter u introduced by O'Brien²⁸, i.e.,

$$g_{||}(T) = g_1 + u(T)g_2, \quad g_{\perp}(T) = g_1 - (\frac{1}{2})u(T)g_2, \quad (8)$$

$$A_{||}(T) = A_1 + u(T)A_2, \quad A_{\perp}(T) = A_1 - (\frac{1}{2})u(T)A_2, \quad (9)$$

where $u(T) \leq 1$. Here, the effects of the zero-point motion have been ignored; i.e., $u(4.2)$ has been assumed to be unity. The values of g_1 , g_2 , A_1 , and A_2 obtained from the 4.2-K data (see Table V) may then be used with one of the measured EPR parameters at a higher temperature to estimate $u(T)$. Since $|g_{||} - g_1| > |g_{\perp} - g_1|$, most precise estimates of $u(T)$ were obtained from the experimental values of $g_{||}(T)$. The remainder of Eqs. (8) and (9) was then used to estimate theoretical values of $g_{\perp}(T)$, $A_{||}(T)$, and $A_{\perp}(T)$. The results for a number of temperatures are given in Table VI for both relative signs of $A_{||}$ and A_{\perp} . Again, agreement with experiment was obtained only for $A_{||}A_{\perp} < 0$, which is consistent with the previous determination, based on the magnitude of the Fermi-contact parameter κ . While $|A_{||}(T)|$ decreased with increasing temperature for both relative signs, the values for $A_{||}A_{\perp} < 0$ were much closer to experiment. Furthermore $|A_{\perp}(T)|$ was found to decrease with increasing tempera-

TABLE V. Calculated parameters for Cu^{2+} in $\text{ZnTiF}_6 \cdot 6\text{H}_2\text{O}$ at 4.2 K. Part (a) shows parameters obtained from the measured g values and the assumption that $\lambda/\Delta = 0.069 \text{ cm}^{-1}$. Part (b) shows parameters obtained from the hyperfine structure measurements assuming $A_{||}$ to be negative and A_{\perp} to be positive. (The values obtained assuming both $A_{||}$ and A_{\perp} to be negative are given in parentheses.)

(a)			
g_1	g_2	q	α^2
2.22	0.24	0.50	0.88
(b)			
A_1 (10^{-4} cm^{-1})	A_2 (10^{-4} cm^{-1})	P (10^{-4} cm^{-1})	κ
-15	-91	420	0.26
(-55)	(-51)	(240)	(0.46)

TABLE VI. "Anisotropy parameter" $u(T)$ and calculated spin-Hamiltonian parameters [obtained from $g_{\parallel}(T)$ and the 4.2-K data using Tables I and II] compared with experiment for $A_{\parallel}A_{\perp} < 0$. (Values in parentheses are for $A_{\parallel}A_{\perp} > 0$.)

T (K)	$u(T)$	g_{\perp}	Calculated		Experimental ^a		
			$ A_{\parallel} $ (10^{-4} cm^{-1})	$ A_{\perp} $ (10^{-4} cm^{-1})	g_{\parallel}	g_{\perp}	$ A_{\parallel} $ (10^{-4} cm^{-1})
146	0.48	2.16	59 (80)	7 (43)	2.335	2.16	54
102 ^b	0.63	2.145	72 (87)	10 (39)	2.37	2.14	67
96	0.79	2.125	87 (95)	17 (35)	2.41	2.13	78
77	0.88	2.115	95 (100)	21 (33)	2.43	2.12	88
4.2	1.00	2.10	106 (106)	30 (30)	2.47	2.10	106

^aExperimental data are taken from Tables I and II.

^b120-K values are an average of the 125-K data for plane 1 and the 115-K data for plane 2.

ture for $A_{\parallel}A_{\perp} < 0$, and, contrary to observation to increase for $A_{\parallel}A_{\perp} > 0$.

The experimental values of the parameter $u(T)$ given in Table VI can be fitted roughly to an exponential dependence of the form

$$u(T) = 1 - \exp(-E/kT), \quad (10)$$

where E represents an activation energy of approximately 100 cm^{-1} .

The temperature dependence of $u(T)$ should depend both on the reorientation time τ between the three tetragonally distorted configurations of the Jahn-Teller effect¹ and on the energy differences between them produced by the low-symmetry components of the crystal field. While the approximate fit of $u(T)$ to an activation energy $E \simeq 100 \text{ cm}^{-1}$ in Eq. (10) may be accidental, it would appear plausible to associate E with the energy difference between the distorted configurations of lowest energy and the other two configurations, which if energetically equivalent would lead to a motionally averaged EPR spectrum of axial symmetry for a given Cu^{2+} ion.²⁹ The gradual change of the EPR spectrum over a wide range of temperatures found in $\text{ZnTiF}_6 \cdot 6\text{H}_2\text{O}$ was not present in the Cu^{2+} spectra of systems of higher symmetry, such as $\text{ZnSiF}_6 \cdot 6\text{H}_2\text{O}$,⁸ $\text{Ca}(\text{OH})_2$,³⁰ and NaCl ,³¹ in which the three distorted configurations are energetically equivalent. This is also the case in $\text{ZnTiF}_6 \cdot 6\text{H}_2\text{O}$ above the structural tran-

sition temperature T_c , so that a sharp transition to a single-line spectrum might be expected on warming the crystal through T_c . It should be noted that for $\text{MgSiF}_6 \cdot 6\text{H}_2\text{O}$, in which the phase transition is near room temperature,⁹ there is a smooth change on cooling from a single-line to a multiline Cu^{2+} spectrum.³²

Höck and Thomas³³ have considered the theoretical problem of the coupling of the 2E orbital ground state to the soft mode of the structural phase transition, showing that a gradual change from a weak to a strong Jahn-Teller effect should occur as the structural phase transition temperature is approached from above. The occurrence in our samples of a concentration-dependent transition temperature occurring well below T_c for pure $\text{ZnTiF}_6 \cdot 6\text{H}_2\text{O}$ (see Sec. II A) is probably due to the strains induced in the crystal by the Cu impurity.³⁴

ACKNOWLEDGMENTS

One of the authors, (D.K.D.) wishes to acknowledge partial support from the Welch Foundation and the Dean of Science of the University of Texas at Arlington. Another author (R.S.R.) wishes to acknowledge the Graduate School of the University of Texas at Arlington for a summer stipend award. The authors wish to thank Dr. F. S. Ham, Dr. N. Fazleyev, and Dr. G. E. Fletcher for helpful comments.

¹See, for example, F. S. Ham, in *Electron Paramagnetic Resonance*, edited by S. Geschwind (Plenum, New York, 1972), pp. 1–119.

²B. Bleaney and D. J. E. Ingram, Proc. Phys. Soc. London Sect. A **63**, 408 (1950).

³B. Bleaney and K. D. Bowers, Proc. Phys. Soc. London Sect. A **65**, 667 (1952).

⁴B. Bleaney, K. D. Bowers, and R. S. Trenam, Proc. R. Soc.

London Ser. A **228**, 157 (1955).

⁵S. Ray, A. Zalkin, and D. H. Templeton, Acta Crystallogr. Sect. B **29**, 2741 (1973).

⁶See, for example, R. W. G. Wyckoff, *Crystal Structures*, 2nd ed. (Interscience, New York, 1965), Vol. 3, pp. 796 and 797.

⁷A. Abragam and M. H. L. Pryce, Proc. Phys. Soc. London Sect. A **63**, 409 (1950).

⁸L. S. Dang, R. Buisson, and F. I. B. Williams, J. Phys. (Paris)

- ⁹S. Syoyama and K. Osaki, *Acta Crystallogr. Sect. B* **28**, 2626 (1972).
- ¹⁰W. C. Hamilton, *Acta Crystallogr.* **15**, 353 (1962).
- ¹¹M. L. Afanasyev, A. F. Lybzikov, V. V. Menshikov, and E. P. Zeer, *Chem. Phys. Lett.* **60**, 279 (1979).
- ¹²R. S. Rubins, *Chem. Phys. Lett.* **28**, 273 (1974).
- ¹³R. S. Rubins and K. K. Kwee, *J. Chem. Phys.* **66**, 3948 (1977).
- ¹⁴R. S. Rubins, *J. Chem. Phys.* **60**, 4189 (1974).
- ¹⁵R. S. Rubins and H. R. Fetterman, *J. Chem. Phys.* **71**, 5163 (1979).
- ¹⁶A. S. Brill and J. H. Venable, Jr., *J. Mol. Biol.* **36**, 343 (1968).
- ¹⁷See, for example, A. Abragam and B. Bleaney, *Electron Paramagnetic Resonance of Transition Ions*, 1st ed. (Clarendon, Oxford, 1970), pp. 455 and 466.
- ¹⁸Sample analyses were made by Galbraith Laboratories, Inc., P. O. Box 4187, Knoxville, Tennessee 37921.
- ¹⁹K. A. Müller, in *Magnetic Resonance and Relaxation*, edited by R. Blinc (North-Holland, Amsterdam, 1974), p. 192.
- ²⁰J. C. Slonczweski, *Phys. Rev.* **131**, 1596 (1963).
- ²¹L. A. Boatner, R. W. Reynolds, Y. Chen, and M. M. Abraham, *Phys. Rev. B* **16**, 86 (1977).
- ²²See, for example, A. H. Maki and B. R. McGarvey, *J. Chem. Phys.* **29**, 31 (1958).
- ²³R. Pappalardo, *J. Mol. Spectrosc.* **6**, 554 (1961).
- ²⁴T. Dreisch and W. Trommer, *Z. Phys. Chem. B* **37**, 37 (1937).
- ²⁵D. Kivelson and R. Neiman, *J. Chem. Phys.* **35**, 149 (1961).
- ²⁶J. F. Gibson, D. J. E. Ingram, and D. Schonland, *Discuss. Faraday Soc.* **26**, 72 (1958).
- ²⁷B. Bleaney, K. D. Bowers, and M. H. L. Pryce, *Proc. R. Soc. London Ser. A* **228**, 166 (1955).
- ²⁸M. C. M. O'Brien, *Proc. R. Soc. London Ser. A* **281**, 323 (1964).
- ²⁹F. S. Ham (private communication).
- ³⁰R. G. Wilson, F. Haluj, and N. E. Hedgecock, *Phys. Rev. B* **1**, 3609 (1970).
- ³¹R. E. Borcherts, H. Kanzaki, and H. Abe, *Phys. Rev. B* **2**, 23 (1970).
- ³²L. N. Tello, M. S. thesis, University of Texas at Arlington, 1983 (unpublished).
- ³³K. H. Höck and H. Thomas, in *Electron-Phonon Interactions and Phase Transitions*, edited by T. Riste (Plenum, New York, 1977), pp. 271–276.
- ³⁴See, for example, A. N. Das and B. Ghosh, *J. Phys. C* **16**, 102 (1983).